Archival Report

Biological Psychiatry: CNNI

Distinct Patterns of Atypical Functional Connectivity in Lower-Functioning Autism

Maya A. Reiter, Lisa E. Mash, Annika C. Linke, Christopher H. Fong, Inna Fishman, and Ralph-Axel Müller

ABSTRACT

BACKGROUND: Functional magnetic resonance imaging research on autism spectrum disorders (ASDs) has been largely limited to individuals with near-average intelligence. Although cognitive impairment is common in ASDs, functional network connectivity in this population remains poorly understood. Specifically, it remains unknown whether lower-functioning individuals exhibit exacerbated connectivity abnormalities similar to those previously detected in higher-functioning samples or specific divergent patterns of connectivity.

METHODS: Resting-state functional magnetic resonance imaging data from 88 children (44 ASD, 44 typically developing; average age: 11 years) were included. Based on IQ, individuals with ASDs were assigned to either a lower-functioning group (mean IQ = 77 $\pm$ 6) or a higher-functioning group (mean IQ = 123 $\pm$ 8). Two typically developing comparison groups were matched to these groups on head motion, handedness, and age. Seeds in the medial prefrontal cortex, posterior cingulate cortex, posterior superior temporal sulcus, insula, and amygdala were used to contrast whole-brain functional connectivity across groups.

RESULTS: Lower-functioning ASD participants (compared with higher-functioning ASD participants) showed significant underconnectivity within the default mode network and the ventral visual stream. Higher-functioning ASD participants (compared with matched typically developing participants) showed significantly decreased anticorrelations among default mode, salience, and task-positive regions. Effect sizes of detected differences were large (Cohen's $d > 1.46$).

CONCLUSIONS: Lower- and higher-functioning individuals with ASDs demonstrated distinct patterns of atypical connectivity. Findings suggest a gross pattern of predominantly reduced network integration in lower-functioning ASDs (affecting default mode and visual networks) and predominantly reduced network segregation in higher-functioning ASDs. Results indicate the need for stratification by general functional level in studies of functional connectivity in ASDs.

Keywords: Autism spectrum disorder, Functional MRI, Intelligence, Low-functioning autism, Neural networks, Neuropsychiatry

https://doi.org/10.1016/j.bpsc.2018.08.009

Functional magnetic resonance imaging (fMRI) research on autism spectrum disorders (ASDs) has primarily focused on samples of individuals with full-scale intelligence quotient (FSIQ) scores around or above average. Unfortunately, such samples misrepresent the true distribution of cognitive abilities in this population (1). The Centers for Disease Control and Prevention (2) estimates that 31% of individuals with ASDs have an intellectual disability (IQ $\leq$ 70), with an additional 23% functioning in the borderline range [71 $\leq$ FSIQ $\leq$ 85 (3)]. However, only a small proportion of ASD cases (roughly 11%, and even fewer when considering data quality) in the Autism Brain Imaging Data Exchange (ABIDE I and II) obtained FSIQ scores $\leq$ 85 (4,5). Imaging research in lower-functioning individuals is a pressing priority for public health (6). Although this segment of the autism spectrum population experiences the most significant impairments, little is known about specific brain anomalies associated with a low general level of functioning in ASDs. Moreover, theories attempting to characterize the neural abnormalities contributing to ASDs are likely incomplete if derived from studies of unrepresentative higher-functioning samples. Inclusion of more representative samples may allow for stronger theory-driven hypotheses in future research.

Resting-state fMRI (rsfMRI) is widely used to study brain function in the absence of an explicit task. rsfMRI detects intrinsic (task-independent) low-frequency fluctuations of the blood oxygen level–dependent signal that are synchronized within functional brain networks (7,8). One advantage of rsfMRI in the study of lower-functioning ASD (L-ASD) individuals is the absence of any task-related confounds (e.g., engagement, performance). However, obtaining high-quality rsfMRI data from this population is challenging because even submillimeter amounts of motion may confound detected blood oxygen level–dependent signal correlations (9). L-ASD individuals are

SEE COMMENTARY ON PAGE 216

ISSN: 2451-9022

often apprehensive of the scanning environment and may struggle to remain still during scans (10,11), especially in the absence of a distracting video or task (12). While improved behavioral protocols combined with advanced MRI sequences can lead to higher success rates in data acquisition (10,11), data-sharing initiatives remain essential for obtaining samples with sufficient statistical power in this population.

Atypical functional connectivity has been detected in many fMRI studies of ASDs (13,14). However, to our knowledge, no previous intrinsic functional connectivity (iFC) studies have focused specifically on L-ASD individuals. We selected five regions of interest commonly linked to atypical connectivity in the ASD iFC literature as seed regions for iFC analyses (13). Atypical connectivity of the default mode network (DMN) in ASDs has been widely reported (15), with many studies showing underconnectivity between anterior (medial prefrontal cortex [mPFC]) and posterior (posterior cingulate cortex [PCC]) midline hubs of the DMN in ASDs (16–22). The DMN is a task-negative network that is active during rest and deactivated during tasks requiring directed attention (23). Anticorrelation between task-negative DMN and task-positive networks marks higher cognitive function in typically developing (TD) populations (24) and is attenuated in many clinical disorders, including ASDs, depression, and neurodegenerative disease (23,25,26). Notably, diminished anticorrelation between task-positive networks and task-negative networks has been reported during tasks (27) and at rest (28) in ASDs. The anterior insula, a key hub of the salience network (SN), has been found to coordinate switching between task-positive networks and task-negative networks in TD individuals (29)—a mechanism that may be affected in ASDs (30). The amygdala (31) and posterior superior temporal sulcus (32) have also been considered of key relevance in ASDs. The amygdala has been implicated in abnormal face processing (33), sensory sensitivity (34), and negative valence (35). Atypical anatomical development and functional connectivity of the posterior superior temporal sulcus (pSTS) have been linked to impaired social cognition in ASDs (36–38).

The current study aimed to take a first step toward filling the large gap in the neuroimaging literature on iFC in L-ASD. The extensive iFC literature on ASDs has not generated a clear picture of the relationship between cognitive abilities and iFC, with only few published studies directly examining FSIQ-related effects. For example, Anderson *et al.* (39) used machine learning to build a diagnostic classifier (including DMN regions, superior parietal lobule, fusiform gyrus, and anterior insula), which was significantly correlated with verbal (but not performance) IQ. However, in a much larger sample (N = 964, mean performance IQ = 106), Nielsen *et al.* (40) presented a classifier (involving similar regions) that showed only weak correlation with verbal IQ (r = −.07) and performance IQ (r = −.03). FSIQ has predominantly been studied as a nuisance variable in studies of individuals of near-average FSIQ [e.g., (21,41), both reporting no IQ effects on results].

In samples predominantly including individuals with near-average FSIQ, effects of general level of cognitive functioning may remain undetected, especially given numerous other factors of variability related to etiological heterogeneity, demography, and treatment history. In the current study, we therefore opted to contrast the tails of the FSIQ distribution in available ASD datasets—that is, participants with FSIQs ≤ 85 and ≥ 115 [1 SD below and above the mean (3)]—to better isolate links between general functional abilities and functional network connectivity in ASDs.

To help understand iFC differences between the L-ASD and higher-functioning ASD (H-ASD) groups, we also tested these groups against suitable TD comparison groups (with differing FSIQ levels). In the absence of previous findings to guide predictions, a default hypothesis was that connectivity patterns differentiating ASD from TD samples would be aggravated in L-ASD participants. However, we also anticipated the possibility of distinctive patterns of atypical iFC found only in L-ASD (but not H-ASD) participants. Such insight into differing iFC patterns could ultimately inform targeted interventions for more severely affected individuals with ASDs.

METHODS AND MATERIALS

Participants

Participants were 88 (44 ASD and 44 TD) children and adolescents, aged 6 to 15 years, selected from in-house data and two other sites contributing to ABIDE II (4). Participants were split into four groups, each comprising 22 individuals: L-ASD, H-ASD, A-TD (average FSIQ TD), and H-TD (higher-FSIQ TD). Participant demographics are shown in Table 1. For in-house data (n = 9 per group), ASD diagnosis was confirmed using expert clinical judgment in conjunction with the Autism Diagnostic Observation Schedule, Second Edition (42,43) and the Autism Diagnostic Interview–Revised (44). Diagnostic labels from the ABIDE databases were retained. Inclusion criteria for ABIDE sites were 1) contribution of >5 L-ASD individuals in the eligible age range with usable anatomical and rsfMRI data (see details below) and 2) rsfMRI data acquired while participants' eyes were open [given effects of eye status on iFC (45)]. Only two sites from ABIDE II [and none from ABIDE I (5)] met these criteria: New York University, group 1 (n = 7 per group), and Oregon Health and Sciences University (n = 6 per group). All ASD individuals from these sites with usable rsfMRI data and FSIQ ≤ 85 were included in the L-ASD group. The H-ASD, H-TD, and A-TD groups were matched to the L-ASD group on age, gender, handedness, and head motion. To minimize potential effects of scanning site, all groups were also matched for age and motion within individual sites (Supplemental Tables S1–S3). Participants in the H-ASD and H-TD groups had FSIQ ≥ 115, but due to matching constraints, 3 of 22 ASD participants and 4 of 22 TD participants with slightly lower scores (between 106 and 114) needed to be included. FSIQ matching could not be reasonably implemented for the L-ASD group because individuals with FSIQ ≤ 85 might not be considered "typically developing" (46). Therefore, an A-TD group was included for further comparison, and a secondary analysis controlling for FSIQ was performed for the contrast of this group with the L-ASD group. This strategy is common in the study of developmental disorders that negatively affect FSIQ such as fetal alcohol syndrome (47).

Ethical Considerations. The in-house study was approved by the San Diego State University and University of California, San Diego, Institutional Review Boards, and all

Table 1. Participant Demographics

All Sites	Age Mean (SD) [Min–Max]	FSIQ Mean (SD) [Min–Max]	RMSD Mean (SD) [Min–Max]	ADOS Total Mean (SD) [Min–Max]	Left Handed *n* (%)	Female *n* (%)
L-ASD (*n* = 22)	11.1 (2.7) [7–15.5]	77 (6) [61–85]	.070 (.030) [.017–.133]	14 (5) [5–24]	4 (19.0)[a]	4 (18.2)
H-ASD (*n* = 22)	11.1 (2.8) [7–15]	123 (8) [106–138]	.068 (.025) [.032–.106]	11 (4) [6–21]	2 (9.1)	3 (13.6)
A-TD (*n* = 22)	11.0 (2.8) [6–15]	99 (7) [88–112]	.064 (.025) [.030–.141]	–	2 (9.1)	7 (31.8)
H-TD (*n* = 22)	10.8 (2.0) [8–14]	124 (8) [108–144]	.064 (.019) [.033–.097]	–	1 (4.5)	5 (22.7)

ADOS, Autism Diagnostic Observation Schedule, Second Edition; A-TD, average FSIQ typically developing; FSIQ, full-scale intelligence quotient; H-ASD, higher-functioning autism spectrum disorder; H-TD, higher FSIQ typically developing; L-ASD, lower-functioning autism spectrum disorder; RMSD, root mean square displacement.

[a]The handedness data point was not available for 1 participant in the L-ASD group.

participants provided informed consent to partake in this research. See Supplemental Table S4 for a description of MRI scanning parameters at each site.

rsfMRI Preprocessing

The first five volumes of each resting-state scan were discarded for T1 equilibration. Images were preprocessed using AFNI (48) (http://afni.nimh.nih.gov) and FSL 5.0 (49) (http://www.fmrib.ox.ac.uk/fsl) suites. In-house rsfMRI data were field map corrected and slice time corrected, and all data were motion corrected and resampled to Montreal Neurological Institute (MNI) 152 3-mm isotropic standard space using FSL's FLIRT (functional to anatomical) and FNIRT (anatomical to standard) normalization tools. Images were spatially smoothed to a global full width at half maximum of 6 mm and temporally smoothed using a bandpass filter of $.008 < f < .08$ Hz. Subject-level regression of 16 nuisance variables was performed for denoising. Regressors included six rigid body motion parameters estimated during motion correction and mean time series from white matter and ventricular cerebrospinal fluid masks obtained from FSL's FAST, eroded by one voxel, each with a first derivative. All 16 nuisance regressors were bandpass filtered using the same second-order Butterworth filter ($.008 < f < .08$ Hz) (50) used for temporal smoothing of the functional images. In addition, individual volumes with framewise displacement $> .5$ mm were censored. Time-series segments with <10 contiguous time points after censoring were also removed. Only participants with at least 80% of volumes retained after censoring were included in analyses, except for one participant (79% retained volumes), whose data were retained for matching purposes. All four groups were well matched on root mean square displacement, a summary measure of motion throughout the scan (Tables 1 and 2).

Seeds

Left and right amygdala masks were created using the Harvard–Oxford subcortical atlas and thresholded at 50% probability. Location and volume of other seeds was determined based on relevant literature (as cited). Left and right anterior insula seeds were 8-mm-radius spheres centered around MNI coordinates ($x = \pm 39$, $y = 23$, $z = -4$) (51). Left and right pSTS seeds were 10-mm-radius spheres centered at MNI coordinates ($x = \pm 47$, $y = -60$, $z = 4$) (37). DMN seeds (mPFC and PCC) were 6-mm-radius spheres centered around MNI coordinates ($x = 0$, $y = 50$, $z = 0$ [mPFC]) and ($x = -6$, $y = -50$, $z = 36$ [PCC]) located in the anterior and posterior DMN midline nodes, as identified by independent component analysis of a sample of nearly 30,000 human subjects (52).

Statistical Analysis

We tested for differences in whole-brain functional connectivity across four contrasts of interest (Supplemental Figure S1): 1) L-ASD versus H-ASD, 2) L-ASD versus A-TD, 3) H-ASD versus H-TD, and 4) A-TD versus H-TD. This design was implemented to address the guiding question of this study: is atypical iFC simply more pronounced in L-ASD than in H-ASD, or do individuals with L-ASD show distinct patterns of iFC?

Mean time series were extracted from the mPFC, PCC, bilateral pSTS, bilateral amygdala, and bilateral insula and were correlated with all other voxels in the brain for each participant (Supplemental Figure S2a–h). Across comparison groups, differences in iFC between the seed region and all other brain voxels were examined using *t* tests implemented by AFNI's 3dttest++. A gray matter mask was used to constrain all analyses to gray matter, cerebellum, and brainstem (excluding white matter and cerebrospinal fluid). We controlled for type I error in accordance with recent recommendations (53) addressing concerns regarding inflated false-positive rates in fMRI research (54). A voxelwise threshold for significance was set at $\alpha < .005$, and the additional cluster size thresholds (number of contiguous significant voxels) were determined using permutation testing with AFNI's 3dttest++ function and the Clustsim argument (Supplemental Table S5).

RESULTS

We found significant iFC differences for the contrasts L-ASD versus H-ASD, L-ASD versus A-TD, and H-ASD versus H-TD but not for A-TD versus H-TD (Table 3 and Figure 1). Overall, significant findings were robust across the three scanning sites, and inclusion of a site covariate did not change the results presented below. No significant iFC differences were detected for the amygdala seeds. See Supplemental Figures S2 to S4 for group-average connectivity

Table 2. Participant *t* Tests

	Group 1	Group 2	Age *t*, *p*	FSIQ *t*, *p*	RMSD *t*, *p*	Sex χ^2, *p*	Handedness[a] χ^2, *p*	ADOS Total *t*, *p*
Contrast 1	L-ASD	H-ASD	−0.001, .99	−20.98, < .001[b]	0.23, .82	0.17, .68	0.89, .35	2.56, .02[b]
Contrast 2	L-ASD	A-TD	0.013, .90	−11.65, < .001[b]	0.77, .44	1.09, .30	0.89, .35	–
Contrast 3	H-TD	H-ASD	−0.40, .69	0.41, .68	−0.70, .49	0.61, .43	0.36, .55	–
Contrast 4	H-TD	A-TD	−0.28, .78	10.89, < .001[b]	−0.030, .98	0.46, .50	0.36, .55	–

ADOS, Autism Diagnostic Observation Schedule, Second Edition; A-TD, average FSIQ typically developing; FSIQ, full-scale intelligence quotient; H-ASD, higher-functioning autism spectrum disorder; H-TD, higher FSIQ typically developing; L-ASD, lower-functioning autism spectrum disorder; RMSD, root mean square displacement.

[a]The handedness data point was not available for 1 participant in the L-ASD group.

[b]$p < .05$.

maps for all seeds (Supplemental Figure S2a–h), scatterplots illustrating data results by site (Supplemental Figure S3a–c), and scatterplots depicting connectivity across all four groups for clusters of significant group differences (Supplemental Figure S4a–c).

Contrast 1: H-ASD Versus L-ASD

Compared with the H-ASD group, the L-ASD group showed significant underconnectivity between the mPFC seed and precuneus/posterior cingulate gyrus (Figure 1). However, within the L-ASD group, no corresponding correlation between FSIQ and functional connectivity was detected in post hoc analysis. Underconnectivity was also observed bilaterally between the pSTS seeds and pericalcarine cortex. These effects were significant with and without controlling for symptom severity (Autism Diagnostic Observation Schedule, Second Edition, total score) (see Supplemental Figure S5). No inverse effects of significantly increased connectivity in the L-ASD group were detected.

Contrast 2: L-ASD Versus A-TD

The L-ASD group showed mPFC overconnectivity with pericalcarine cortex compared with A-TD participants, who showed mostly negative correlations between these regions. This group difference remained significant after controlling for FSIQ (Supplemental Figure S6). Because this result spatially overlapped with the underconnectivity cluster for the pSTS seeds in contrast 1, we tested the correlation between the two

Table 3. Group Differences in Seed to Whole-Brain Functional Connectivity

Contrast	Seed	Size	Peak *t*	Peak β	mm x	mm y	mm z	Mean *z*[a] (SD[a])	Mean *z*[b] (SD[b])	Cohen's *d*	Peak Regions
L-ASD[a] (*n* = 22) vs. H-ASD[b] (*n* = 22)	mPFC	104	−4.45	−.36	8	−50	30	.20 (.13)	.46 (.20)	1.54	Precuneus
	Left pSTS	566	−5.03	−.38	−12	−80	42	.03 (.13)	.25 (.10)	1.90	Cuneal cortex (other: pericalcarine cortex)
		70	−4.69	−.36	−18	−86	24	.12 (.18)	.39 (.17)	1.54	Left lateral occipital cortex, superior division
	Right pSTS	340	−4.91	−.45	24	−86	36	.08 (.12)	.32 (.12)	2.00	Right lateral occipital cortex, superior division (other: cuneal cortex, pericalcarine cortex)
L-ASD[a] (*n* = 22) vs. A-TD[b] (*n* = 22)	mPFC	127	4.34	.28	8	−78	16	.16 (.15)	−.06 (.15)	1.46	Cuneal cortex (other: pericalcarine cortex)
H-ASD[a] (*n* = 22) vs. H-TD[b] (*n* = 22)	PCC	90	4.93	.36	30	54	28	.10 (.14)	−.15 (.16)	1.66	Right superior frontal gyrus
		85	4.77	.30	38	16	−8	.00 (.14)	−.22 (.11)	1.75	Right insula
		75	4.63	.31	−34	−72	−26	.09 (.12)	−.13 (.11)	1.91	Left crus I
	Right insula	164	4.24	.28	2	−56	18	.01 (.15)	−.22 (.15)	1.53	Precuneus (other: posterior cingulate cortex)

All clusters reported were significant at the criterion threshold of alpha = .05 ($p < .005$, voxel extent). Cluster size is reported in voxels (3-mm isotropic resolution). The *t* score, value, and Montreal Neurological Institute mm coordinates are reported for the peak voxel of the cluster (columns 4–8). Group-level parameter estimates (mean and SD) of clusterwise mean *z* scores are reported (columns 9 and 10). Cohen's *d* is reported for each cluster as an estimated effect size. Peak regions were labeled using the Talairach and Harvard–Oxford cortical and subcortical atlases. For large clusters, other regions covered by the cluster are reported in parentheses. Supplemental Figures S5 and S6 present results for the L-ASD vs. H-ASD contrast with Autism Diagnostic Observation Schedule total entered as a covariate and for the L-ASD vs. A-TD contrast with FSIQ included in the model as a covariate.

A-TD, average FSIQ typically developing; FSIQ, full-scale intelligence quotient; H-ASD, higher-functioning autism spectrum disorder; H-TD, higher FSIQ typically developing; L-ASD, lower-functioning autism spectrum disorder; mPFC, medial prefrontal cortex; PCC, posterior cingulate cortex; pSTS, posterior superior temporal sulcus.

[a]Group 1.

[b]Group 2.

effects in the L-ASD group. Pearson correlation showed no association ($r = -.142$, $t = -0.63$, $p = .54$).

Contrast 3: H-ASD Versus H-TD

Compared with the H-TD group, the H-ASD group showed significantly greater connectivity between the PCC and right superior frontal gyrus (SFG), right anterior insula, and left crus I of the cerebellum. However, within the H-ASD group, no corresponding correlations between FSIQ and these functional connectivity patterns were detected post hoc. Significant group differences in iFC between the PCC and right SFG and left crus I reflected a shift from mostly negative to mostly positive connectivity in the H-ASD group compared with the H-TD group. Group differences in iFC between the PCC and right insula were driven by mostly negative iFC in the H-TD group but near-zero iFC scores in the H-ASD group.

Post Hoc Analyses

H-ASD Versus A-TD. Because in the main contrasts the two ASD groups were compared with different TD groups, we performed a supplementary analysis contrasting the H-ASD group with the A-TD group (the same TD group as in contrast 2). Unlike the mPFC–pericalcarine overconnectivity observed in the L-ASD versus A-TD comparison, the H-ASD group showed mPFC overconnectivity with the right inferior frontal gyrus extending into the insular cortex (Supplemental Figure S7).

Interactions With Symptom Severity. We investigated whether seed-to-whole-brain functional connectivity related differently to ASD symptom severity (Autism Diagnostic Observation Schedule, Second Edition, total scores) in the L-ASD versus H-ASD groups. We found no significant interactions in the relationship between symptom severity and seed-to-whole-brain functional connectivity in the L-ASD versus H-ASD groups.

Age Effects. Linear regression showed no significant relationships between age and functional connectivity between the regions presented above across the entire sample (Supplemental Table S6). In addition, there were no age by diagnosis (ASD vs. TD) or age by functioning level (H-ASD vs. L-ASD) interactions with functional connectivity (Supplemental Tables S7 and S8).

DISCUSSION

Although hundreds of imaging studies have examined intrinsic functional connectivity in individuals with ASDs with average or above-average intelligence, no systematic research on lower-functioning segments of the ASD population is available. The current study has taken a first step toward filling this knowledge gap by examining a multisite sample of exclusively lower-functioning individuals (FSIQ $\leq$ 85). Our primary research question, whether L-ASD individuals would simply show more severe forms of the same regional patterns of atypical iFC as seen in higher-functioning individuals (H-ASD), could be answered in the negative. In fact, L-ASD participants showed extensive differences in iFC, for several seed regions, in direct comparison with the H-ASD group. Moreover, the L-ASD and H-ASD groups showed distinct patterns of atypical connectivity with the mPFC compared with an A-TD group. Finally, in comparison with the FSIQ-matched H-TD group, the H-ASD group showed overconnectivity for the PCC and right insula in regions that showed more neurotypical levels of iFC in the L-ASD group (Supplemental Figure S4c). These findings strongly suggest that L-ASD is characterized by distinctive patterns of atypical network organization rather than simply more of the same abnormalities detected in the many previous studies with mostly higher-functioning participants.

In the L-ASD group, atypical connectivity of lower-order visual cortex was remarkable. Compared with the H-ASD group, L-ASD individuals exhibited underconnectivity within parts of the ventral visual stream and the DMN, suggesting reduced network integration in lower-functioning individuals. However, compared with the TD groups, both ASD groups exhibited internetwork overconnectivity, albeit across different networks. L-ASD individuals exhibited overconnectivity between the DMN and visual regions, whereas the H-ASD group showed overconnectivity between the DMN and SN as well as task-positive regions. Notably, the H-ASD group exhibited mostly diminished anticorrelations compared with H-TD individuals (indicating reduced network segregation) between these networks. Our results also indicate that iFC of lower-order visual cortex is affected in different ways in lower-functioning versus higher-functioning children with ASDs (Supplemental Figure S4a).

In contrast, no significant differences in iFC were found between the two TD groups that differed on FSIQ. FSIQ relationships with iFC, especially involving frontoparietal regions, have been reported for larger samples of TD children [e.g., (55)]. In the current study, which included only smaller TD samples that primarily served as comparison groups with ASD samples, an expected trend toward stronger anticorrelations between the right SFG (part of task-positive frontoparietal network) and PCC (task-negative DMN hub) in the H-TD group compared with the A-TD group was observed. Remarkably, this trend was reversed in ASD, with higher mean iFC in H-ASD samples than in L-ASD samples (Supplemental Figure S4c). The overall pattern of findings further supports the conclusion that a lower general level of functioning in ASDs may be associated with specific alterations in brain network organization.

DMN Underconnectivity in Lower-Functioning Children With ASDs

Independent of ASD symptom severity, the L-ASD group showed reduced connectivity between midline hubs of the DMN when compared with the H-ASD group. (A concordant effect in the comparison L-ASD vs. A-TD group remained below corrected significance.) Underconnectivity between the main DMN nodes (mPFC and PCC) is among the best-replicated imaging findings in previous ASD studies that included mixed samples with mostly higher-functioning participants (16–22,28,56–58). Our findings suggest that DMN underconnectivity findings broadly reported in the literature may have been primarily driven by participants with lower or average IQ, whereas many children with ASDs and above-average intelligence tend to show relatively high levels of

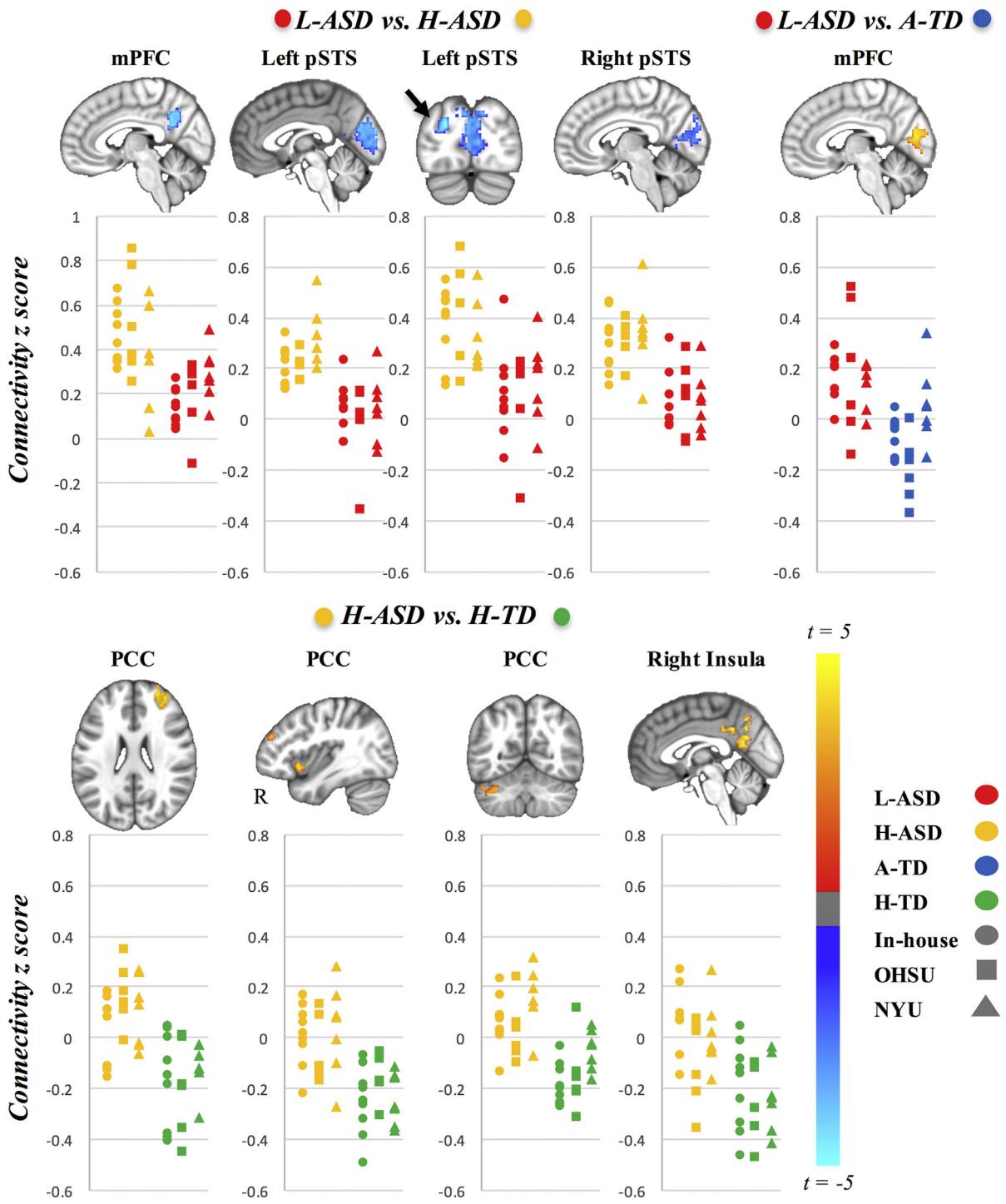

Figure 1. Group differences in functional connectivity. Presented are group differences in seed to whole-brain functional connectivity for contrast 1: lower-functioning ASD (L-ASD) vs. higher-functioning ASD (H-ASD); contrast 2: L-ASD vs. average full-scale intelligence quotient typically developing (A-TD); and contrast 3: H-ASD vs. higher full-scale intelligence quotient typically developing (H-TD). Data are presented in neurological orientation (left = left). Clusters in the panels above denote significant group differences in functional connectivity with the seed listed above (voxelwise $p < .005$, whole-brain cluster corrected at $p < .05$). Scatter plots depicting individual connectivity scores for both groups contrasted are provided for illustrative purposes (H-ASD, yellow; L-ASD, red; H-TD, green; A-TD, blue). The individual symbols used in the scatter plots correspond to the different scanning sites included (circle, in-house; square, Oregon Health and Sciences University (OHSU); triangle, New York University (NYU). There were no significant differences for contrast 4 (A-TD vs. H-TD). mPFC, medial prefrontal cortex; PCC, posterior cingulate cortex; pSTS, posterior superior temporal sulcus.

within-network DMN iFC. Indeed, mean iFC was slightly higher in the H-ASD group when compared with the A-TD and H-TD groups (Supplemental Figure S4a).

Atypical Connectivity of Visual Cortex in L-ASD

Behavioral studies suggest atypical visual processing in ASDs (59), with some islands of superior abilities, for example, in spatial reasoning (60) and visual search [O'Riordan *et al.* (61)]. In addition to pronounced underconnectivity within the DMN, the L-ASD group exhibited lower iFC bilaterally between the pSTS and pericalcarine cortex compared with the H-ASD group. However, the L-ASD group showed overconnectivity between similar visual regions and the anterior DMN hub (mPFC) in comparison with the A-TD group. The pericalcarine cortex is the location of the primary visual cortex surrounding the calcarine fissures in the occipital lobes; this region receives visual input from the thalamus via optic radiations and transmits information to higher-order processing regions. The findings described above are broadly consistent with evidence of the atypical role of the early visual cortex in ASDs (62,63), and more specifically with altered connectivity between the pSTS and lower-order visual cortex (37,38). Our finding of weak iFC between lower-order visual cortices and the pSTS in the L-ASD group may reflect reduced processing along the ventral visual stream, which is important for object identification and higher-order visual processing (64). Specifically, reduced iFC with the pSTS in L-ASD may affect audiovisual integration, biological motion, and face perception as well as—in the left hemisphere—language (32).

In contrast to underconnectivity within the ventral visual stream, the pericalcarine cortex was overconnected with the mPFC in L-ASD participants in comparison with the A-TD group (with a concordant difference in mean iFC in comparison with the H-ASD group) (Supplemental Figure S4b). While further supporting an atypical role of the visual cortex in L-ASD, a functional interpretation of this specific finding is uncertain. No link between this effect and visual–pSTS underconnectivity was found, suggesting that high levels of iFC between the mPFC and visual cortex do not reflect a compensatory mechanism for reduced ventral stream integration in L-ASD. Although atypically increased iFC between the DMN and visual cortex has been reported before in higher-functioning children with ASDs (22,28), these were findings for PCC seeds and not for the anterior DMN hub in the mPFC, as in the current study. More generally, however, increased visual cortex activation (63) and occipital connectivity [Keehn *et al.* (65)] have been reported during cognitive tasks in ASDs.

Functional Networks: Less Integrated in L-ASD, Less Segregated in H-ASD?

It should be noted that for optimal contrast with L-ASD, our H-ASD group represented the upper tail of the FSIQ distribution in ASD neuroimaging studies and therefore differed from cohorts included in most studies [with a mean FSIQ of 123, 1 SD above the mean of the total ASD sample across all sites included in ABIDE (4,5)]. Compared with L-ASD, the H-ASD group had more robust iFC within the DMN and parts of the ventral processing stream, suggesting greater network integration. In contrast, the pattern of differences in comparison with H-TD participants indicated reduced network segregation in the H-ASD group. H-TD participants mostly showed anticorrelations between the posterior DMN hub in the PCC and SN (right insula), a task-positive region in the right SFG, and the left cerebellar crus I, a region that has been related to visual processing (66). These anticorrelations were absent or even reversed in the H-ASD group, suggesting reduced segregation between functionally differentiated networks. Surprisingly, iFC in the L-ASD participants was more similar to the TD groups across all of these clusters (Supplemental Figure S4c).

The overall pattern of our results suggests that previous findings of reduced network integration accompanied by reduced network segregation in ASDs (13,38,67,68) may be differentially driven by individuals with a lower versus higher general level of functioning. While we found evidence of predominantly reduced network integration in L-ASD (lower iFC between nodes of the same network), network anomalies in H-ASD participants predominantly reflected reduced segregation (higher iFC or reduced anticorrelations between networks).

Limitations

As in all studies of ASDs, caution is needed because many factors of variability (e.g., etiological heterogeneity, treatment history) probably also affect network organization and connectivity and could not be controlled in this study. The sample size available from combined scanning sites was relatively small, which limited statistical power. General conclusions regarding the large low-functioning population with ASDs must therefore be drawn with caution, although the consistency of many findings across scanning sites was encouraging. Additional research investigating the relationship between functional connectivity in L-ASD and more specific behavioral measures than FSIQ is warranted.

While previous research has shown atypical effects of age on functional connectivity in ASD (69), we found no effects of age in the current study; it is possible that detection of such effects requires larger samples. Larger studies are also required in order to examine differences in L-ASD across a wider array of brain regions because functional connectivity patterns have been shown to be regionally distinct even when multiple regions are sampled from a single network's hub (70). Usable data were available for only three L-ASD participants with FSIQ < 70. Improved acquisition and analysis protocols permitting inclusion of individuals with intellectual disability will be crucial in future studies because, paradoxically, neuroimaging over the past decades has largely excluded children who have the most severe forms of the disorder and present the most urgent public health need.

Conclusions

Our findings suggest that neural network connectivity in children with ASDs and lower general functional abilities may be associated with distinctly atypical patterns that differ from those found in H-ASDs. Whereas effects detected in relevant comparisons indicated reduced network integration (within the DMN and ventral visual stream) in L-ASD, they showed reduced network segregation (among the DMN, SN, and one task-positive frontal region) in H-ASD. More broadly, our results indicate the need for better stratification of ASD study

designs and analyses with respect to general levels of functioning because the combination of lower- and higher-functioning individuals in most previous studies may have confounded or obscured functional network anomalies.

ACKNOWLEDGMENTS AND DISCLOSURES

The National Institutes of Health supported the acquisition of the in-house datasets (Grant Nos. R01 MH081023 and R01 MH101173 [to R-AM] and Grant No. K01 MH097972 [to IF]). MAR was supported by the Autism Speaks Sir Dennis Weatherstone Fellowship program (Grant No. 10609), and Lisa Mash was supported by a National Science Foundation Graduate Research Fellowship (Grant No. 1321850).

We thank the families who participated in this study and those individuals involved in organizing and contributing to the ABIDE initiatives. We also acknowledge Jingwen Liu for her contributions to the figures presented.

An oral presentation including results of this study was delivered by the first author at the International Society for Autism Research annual conference in May 2018, Rotterdam, The Netherlands.

The authors report no biomedical financial interests or potential conflicts of interest.

ARTICLE INFORMATION

From the San Diego State University/University of California, San Diego Joint Doctoral Program in Clinical Psychology (MAR, LEM, IF, R-AM) and Brain Development Imaging Laboratories (MAR, LEM, ACL, CHF, IF, R-AM), Department of Psychology, San Diego State University, San Diego, California.

Address correspondence to Ralph-Axel Müller, Ph.D., Brain Development Imaging Laboratories, Department of Psychology, San Diego State University, 6363 Alvarado Court, Suite 200, San Diego, CA 92120; E-mail: rmueller@sdsu.edu.

Received May 29, 2018; revised Aug 3, 2018; accepted Aug 10, 2018.

Supplementary material cited in this article is available online at https://doi.org/10.1016/j.bpsc.2018.08.009.

REFERENCES

1. Jack A, Pelphrey KA (2017): Annual research review: Understudied populations within the autism spectrum—Current trends and future directions in neuroimaging research. J Child Psychol Psychiatry 58:411–435.
2. Centers for Disease Control and Prevention (2014): Prevalence of autism spectrum disorder among children aged 8 years—Autism and Developmental Disabilities Monitoring Network, 11 sites, United States, 2010. MMWR Morb Mortal Wkly Rep 63(SS02):2–21.
3. Alloway TP (2010): Working memory and executive function profiles of individuals with borderline intellectual functioning. J Intellect Disabil Res 54:448–456.
4. Di Martino A, O'Connor D, Chen B, Alaerts K, Anderson JS, Assaf M, *et al.* (2017): Data descriptor: Enhancing studies of the connectome in autism using the Autism Brain Imaging Data Exchange II. Sci Data 4:170010.
5. Di Martino A, Yan CG, Li Q, Denio E, Castellanos FX, Alaerts K, *et al.* (2014): The Autism Brain Imaging Data Exchange: Towards a large-scale evaluation of the intrinsic brain architecture in autism. Mol Psychiatry 19:659–667.
6. Chakrabarti B (2017): Commentary: Critical considerations for studying low-functioning autism. J Child Psychol Psychiatry 58:436–438.
7. Biswal B, Yetkin FZ, Haughton VM, Hyde JS (1995): Functional connectivity in the motor cortex of resting human brain using echo-planar MRI. J Magn Reson A 34:537–541.
8. Van Dijk KRA, Hedden T, Venkataraman A, Evans KC, Lazar SW, Buckner RL (2010): Intrinsic functional connectivity as a tool for human connectomics: Theory, properties, and optimization. J Neurophysiol 103:297–321.
9. Power JD, Mitra A, Laumann TO, Snyder AZ, Schlaggar BL, Petersen SE (2014): Methods to detect, characterize, and remove motion artifact in resting state fMRI. NeuroImage 84:320–341.
10. Cox AD, Virues-Ortega J, Julio F, Martin TL (2017): Establishing motion control in children with autism and intellectual disability: Applications for anatomical and functional MRI. J Appl Behav Anal 50:8–26.
11. Nordahl CW, Mello M, Shen AM, Shen MD, Vismara LA, Li DA, *et al.* (2016): Methods for acquiring MRI data in children with autism spectrum disorder and intellectual impairment without the use of sedation. J Neurodev Disord 8:20.
12. Huijbers W, Van Dijk KRA, Boenniger MM, Stirnberg R, Breteler MMB (2016): Less head motion during MRI under task than resting-state conditions. NeuroImage 147:111–120.
13. Hull JV, Dokovna LB, Jacokes ZJ, Torgerson CM, Irimia A, Van Horn JD, , for GENDAAR Research Consortium (2017): Resting-state functional connectivity in autism spectrum disorders: A review. Front Psychiatry 7:205.
14. Mash LE, Reiter MA, Linke AC, Townsend J, Muller RA (2018): Multimodal approaches to functional connectivity in autism spectrum disorders: An integrative perspective. Dev Neurobiol 78:456–473.
15. Padmanabhan A, Lynch CJ, Schaer M, Menon V (2017): The default mode network in autism. Biol Psychiatry Cogn Neurosci Neuroimaging 2:476–486.
16. Assaf M, Jagannathan K, Calhoun VD, Miller L, Stevens MC, Sahl R, *et al.* (2010): Abnormal functional connectivity of default mode sub-networks in autism spectrum disorder patients. NeuroImage 53:247–256.
17. Dichter GS (2012): Functional magnetic resonance imaging of autism spectrum disorders. Dialogues Clin Neurosci 14:319–351.
18. Doyle-Thomas KA, Lee W, Foster NE, Tryfon A, Ouimet T, Hyde KL, *et al.* (2015): Atypical functional brain connectivity during rest in autism spectrum disorders. Ann Neurol 77:866–876.
19. Jung M, Kosaka H, Saito DN, Ishitobi M, Morita T, Inohara K, *et al.* (2014): Default mode network in young male adults with autism spectrum disorder: Relationship with autism spectrum traits. Mol Autism 5:35.
20. Monk CS, Peltier SJ, Wiggins JL, Weng SJ, Carrasco M, Risi S, *et al.* (2009): Abnormalities of intrinsic functional connectivity in autism spectrum disorders. NeuroImage 47:764–772.
21. Weng SJ, Wiggins JL, Peltier SJ, Carrasco M, Risi S, Lord C, *et al.* (2010): Alterations of resting state functional connectivity in the default network in adolescents with autism spectrum disorders. Brain Res 1313:202–214.
22. Yerys BE, Gordon EM, Abrams DN, Satterthwaite TD, Weinblatt R, Jankowski KF, *et al.* (2015): Default mode network segregation and social deficits in autism spectrum disorder: Evidence from non-medicated children. NeuroImage Clin 9:223–232.
23. Raichle ME, MacLeod AM, Snyder AZ, Powers WJ, Gusnard DA, Shulman GL (2001): A default mode of brain function. Proc Natl Acad Sci U S A 98:676–682.
24. Hampson M, Driesen N, Roth JK, Gore JC, Constable RT (2010): Functional connectivity between task-positive and task-negative brain areas and its relation to working memory performance. Magn Reson Imaging 28:1051–1057.
25. Menon V (2011): Large-scale brain networks and psychopathology: A unifying triple network model. Trends Cogn Sci 15:483–506.
26. Whitfield-Gabrieli S, Ford JM (2012): Default mode network activity and connectivity in psychopathology. Annu Rev Clin Psychol 8:49–76.
27. Kennedy DP, Redcay E, Courchesne E (2006): Failing to deactivate: Resting functional abnormalities in autism. Proc Natl Acad Sci U S A 103:8275–8280.
28. Abbott AE, Nair A, Keown CL, Datko M, Jahedi A, Fishman I, *et al.* (2016): Patterns of atypical functional connectivity and behavioral links in autism differ between default, salience, and executive networks. Cereb Cortex 26:4034–4045.
29. Sridharan D, Levitin DJ, Menon V (2008): A critical role for the right fronto-insular cortex in switching between central-executive and default-mode networks. Proc Natl Acad Sci U S A 105:12569–12574.
30. Uddin LQ, Menon V (2009): The anterior insula in autism: Underconnected and under-examined. Neurosci Biobehav Rev 33:1198–1203.

31. Baron-Cohen S, Ring HA, Bullmore ET, Wheelwright S, Ashwin C, Williams SC (2000): The amygdala theory of autism. Neurosci Biobehav Rev 24:355–364.
32. Redcay E (2008): The superior temporal sulcus performs a common function for social and speech perception: Implications for the emergence of autism. Neurosci Biobehav Rev 32:123–142.
33. Aoki Y, Cortese S, Tansella M (2015): Neural bases of atypical emotional face processing in autism: A meta-analysis of fMRI studies. World J Biol Psychiatry 16:291–300.
34. Green SA, Hernandez L, Tottenham N, Krasileva K, Bookheimer SY, Dapretto M (2015): Neurobiology of sensory overresponsivity in youth with autism spectrum disorders. JAMA Psychiatry 72:778–786.
35. Kleinhans NM, Reiter MA, Neuhaus E, Pauley G, Martin N, Dager S, *et al.* (2016): Subregional differences in intrinsic amygdala hyperconnectivity and hypoconnectivity in autism spectrum disorder. Autism Res 9:760–772.
36. Alaerts K, Nayar K, Kelly C, Raithel J, Milham MP, Di Martino A (2015): Age-related changes in intrinsic function of the superior temporal sulcus in autism spectrum disorders. Soc Cogn Affect Neurosci 10:1413–1423.
37. Alaerts K, Woolley DG, Steyaert J, Di Martino A, Swinnen SP, Wenderoth N (2014): Underconnectivity of the superior temporal sulcus predicts emotion recognition deficits in autism. Soc Cogn Affect Neurosci 9:1589–1600.
38. Shih P, Keehn B, Oram JK, Leyden KM, Keown CL, Muller RA (2011): Functional differentiation of posterior superior temporal sulcus in autism: A functional connectivity magnetic resonance imaging study. Biol Psychiatry 70:270–277.
39. Anderson JS, Nielsen JA, Froehlich AL, DuBray MB, Druzgal TJ, Cariello AN, *et al.* (2011): Functional connectivity magnetic resonance imaging classification of autism. Brain 134:3739–3751.
40. Nielsen JA, Zielinski BA, Fletcher PT, Alexander AL, Lange N, Bigler ED, *et al.* (2013): Multisite functional connectivity MRI classification of autism: ABIDE results. Front Hum Neurosci 7:599.
41. Salmi J, Roine U, Glerean E, Lahnakoski J, Nieminen-von Wendt T, Tani P, *et al.* (2013): The brains of high functioning autistic individuals do not synchronize with those of others. NeuroImage Clin 3:489–497.
42. Gotham K, Risi S, Pickles A, Lord C (2007): The Autism Diagnostic Observation Schedule: Revised algorithms for improved diagnostic validity. Rev J Autism Dev Disord 37:613–627.
43. Lord C, Rutter M, DiLavore PC, Risi S, Gotham K, Bishop S (2012): Autism Diagnostic Observation Schedule, Second Edition. Torrance, CA: Western Psychological Services.
44. Lord C, Rutter M, Le Couteur A (1994): Autism Diagnostic Interview–Revised: A revised version of a diagnostic interview for caregivers of individuals with possible pervasive developmental disorders. J Autism Dev Disord 24:659–685.
45. Nair S, Jao Keehn RJ, Berkebile MM, Maximo JO, Witkowska N, Muller RA (2018): Local resting state functional connectivity in autism: Site and cohort variability and the effect of eye status. Brain Imaging Behav 12:168–179.
46. Jarrold C, Brock J (2004): To match or not to match? Methodological issues in autism-related research. Rev J Autism Dev Disord 34:81–86.
47. Crocker N, Riley EP, Mattson SN (2015): Visual-spatial abilities relate to mathematics achievement in children with heavy prenatal alcohol exposure. Neuropsychology 29:108–116.
48. Cox RW (1996): AFNI: Software for analysis and visualization of functional magnetic resonance neuroimages. Comput Biomed Res 29:162–173.
49. Smith SM, Jenkinson M, Woolrich MW, Beckmann CF, Behrens TEJ, Johansen-Berg H, *et al.* (2004): Advances in functional and structural MR image analysis and implementation as FSL. NeuroImage 23: S208–S219.
50. Satterthwaite TD, Elliott MA, Gerraty RT, Ruparel K, Loughead J, Calkins ME, *et al.* (2013): An improved framework for confound regression and filtering for control of motion artifact in the preprocessing of resting-state functional connectivity data. NeuroImage 64:240–256.
51. Uddin LQ, Supekar K, Lynch CJ, Cheng KM, Odriozola P, Barth ME, *et al.* (2015): Brain state differentiation and behavioral inflexibility in autism. Cereb Cortex 25:4740–4747.
52. Smith SM, Fox PT, Miller KL, Glahn DC, Fox PM, Mackay CE, *et al.* (2009): Correspondence of the brain's functional architecture during activation and rest. Proc Natl Acad Sci U S A 106:13040–13045.
53. Cox RW, Chen G, Glen DR, Reynolds RC, Taylor PA (2017): fMRI clustering in AFNI: False-positive rates redux. Brain Connect 7: 152–171.
54. Eklund A, Nichols TE, Knutsson H (2016): Cluster failure: Why fMRI inferences for spatial extent have inflated false-positive rates. Proc Natl Acad Sci U S A 113:7900–7905.
55. Li C, Tian L (2014): Association between resting-state coactivation in the parieto-frontal network and intelligence during late childhood and adolescence. Am J Neuroradiol 35:1150–1156.
56. Joshi G, Gabrieli J, Biederman J, Whitfield-Gabrieli S (2015): Integration and segregation of default mode network resting-state functional connectivity in high-functioning autism spectrum disorder. Eur Neuropsychopharmacol 25:S190–S191.
57. Washington SD, Gordon EM, Brar J, Warburton S, Sawyer AT, Wolfe A, *et al.* (2014): Dysmaturation of the default mode network in autism. Hum Brain Mapp 35:1284–1296.
58. Falahpour M, Thompson WK, Abbott AE, Jahedi A, Mulvey ME, Datko M, *et al.* (2016): Underconnected, but not broken? Dynamic functional connectivity MRI shows underconnectivity in autism is linked to increased intra-individual variability across time. Brain Connect 6:403–413.
59. Simmons DR, Robertson AE, McKay LS, Toal E, McAleer P, Pollick FE (2009): Vision in autism spectrum disorders. Vision Res 49:2705–2739.
60. Stevenson JL, Gernsbacher MA (2013): Abstract spatial reasoning as an autistic strength. PLoS One 8:e5939.
61. O'Riordan MA, Plaisted KC, Driver J, Baron-Cohen S (2001): Superior visual search in autism. J Exp Psychol Hum Percept Perform 27: 719–730.
62. Lundstrom S, Reichenberg A, Anckarsater H, Lichtenstein P, Gillberg C (2015): Autism phenotype versus registered diagnosis in Swedish children: Prevalence trends over 10 years in general population samples. BMJ 350:h1961.
63. Samson F, Mottron L, Soulieres I, Zeffiro TA (2012): Enhanced visual functioning in autism: An ALE meta-analysis. Hum Brain Mapp 33:1553–1581.
64. Ungerleider LG, Haxby JV (1994): "What" and "where" in the human brain. Current Biol 4:157–165.
65. Keehn B, Shih P, Brenner LA, Townsend J, Müller R-A (2013): Functional connectivity for an "island of sparing" in autism spectrum disorder: An fMRI study of visual search. Hum Brain Mapp 34:2524–2537.
66. D'Mello AM, Stoodley CJ (2015): Cerebro-cerebellar circuits in autism spectrum disorder. Front Neurosci 9:408.
67. Fishman I, Datko M, Cabrera Y, Carper RA, Muller RA (2015): Reduced integration and differentiation of the imitation network in autism: A combined functional connectivity magnetic resonance imaging and diffusion-weighted imaging study. Ann Neurol 78:958–969.
68. Rudie JD, Brown JA, Beck-Pancer D, Hernandez LM, Dennis EL, Thompson PM, *et al.* (2013): Altered functional and structural brain network organization in autism. NeuroImage Clin 2:79–94.
69. Nomi JS, Uddin LQ (2015): Developmental changes in large-scale network connectivity in autism. NeuroImage Clin 7:732–741.
70. Lynch CJ, Uddin LQ, Supekar K, Khouzam A, Phillips J, Menon V (2013): Default mode network in childhood autism: Posteromedial cortex heterogeneity and relationship with social deficits. Biol Psychiatry 74:212–219.